

Temperature and Disorder Chaos in Three-Dimensional Ising Spin Glasses

Helmut G. Katzgraber¹ and Florent Krzakala²

¹*Theoretische Physik, ETH Zürich, CH-8093 Zürich, Switzerland*

²*Laboratoire de Physico-Chimie Théorique, UMR CNRS 7083, ESPCI, 10 rue Vauquelin, 75005 Paris, France*

(Received 7 June 2006; published 3 January 2007)

We study the effects of small temperature as well as disorder perturbations on the equilibrium state of three-dimensional Ising spin glasses via an alternate scaling ansatz. By using Monte Carlo simulations, we show that temperature and disorder perturbations yield chaotic changes in the equilibrium state and that temperature chaos is considerably harder to observe than disorder chaos.

DOI: 10.1103/PhysRevLett.98.017201

PACS numbers: 75.10.Nr, 05.50.+q, 75.40.Mg, 75.50.Lk

The fragility of the equilibrium state of random frustrated systems such as the Edwards-Anderson Ising spin glass [1–3] has been predicted a long time ago [4,5] and analyzed on the basis of scaling arguments [6,7]. These scaling arguments predict that the configurations which dominate the partition function change *drastically* and *randomly* when the temperature or the disorder in the interactions between the spins are modified ever so slightly. The *temperature-chaos* and *disorder-chaos* effects have attracted considerable attention both from theory and experiment because of their potential relevance in explaining the spectacular rejuvenation and memory effects observed in hysteresis experiments in spin glasses [8–10] as well as other materials, such as random polymers and pinned elastic manifolds. Although there is evidence of *disorder chaos* in spin glasses, temperature chaos remains a controversial issue [11–15], whereas for random polymers or pinned elastic objects [16] chaos in general is well established [17–19].

Despite this lack of consensus, it has been surmised that temperature chaos would only be observable in spin glasses at very large system sizes and for large temperature changes [20] thus making its presence unfathomable in simulations. These claims have recently been challenged. In particular, recent results point towards the existence of temperature chaos in four-dimensional Ising spin glasses [21] where the free energy of a domain wall induced by a change in boundary conditions changes its sign chaotically with temperature in accordance with the droplet/scaling theory [4,6,7]. In this work we study the overlap between states at different temperatures and disorder distributions *directly* for a *physically relevant* three-dimensional (3D) Ising spin glass. Our results show that the scaling laws that arise from the droplet theory are indeed well satisfied in 3D provided low enough temperatures are considered, although small corrections need to be applied. In addition, we show that temperature and disorder chaos have similar scaling functions. By rescaling the characteristic length scale in the problem, we show that disorder chaos appears at much shorter scales than temperature chaos.

The Letter is organized as follows: We discuss first the model and Monte Carlo methods used, followed by the

disorder- and temperature-chaos scaling approaches. We conclude with the results of our simulations of the 3D Ising spin glass and a general discussion.

Model and numerical method.—The Edwards-Anderson [1] Ising spin glass is given by the Hamiltonian

$$\mathcal{H} = -\sum_{\langle ij \rangle} J_{ij} S_i S_j, \quad (1)$$

where the Ising spins $S_i \in \{\pm 1\}$ are on a cubic lattice with $N = L^3$ vertices and the interactions J_{ij} are Gaussian distributed random numbers with zero mean and standard deviation unity. The sum is over nearest neighbor pairs. The model undergoes a spin-glass transition at $T_c = 0.951(9)$ [22–24].

The order parameter of the system is defined via the overlap between two copies α and β , i.e.,

$$q_{\alpha,\beta} = \frac{1}{N} \sum_{i=1}^N S_i^\alpha S_i^\beta. \quad (2)$$

Following previous studies [11,12], we probe temperature chaos when the temperature between both replicas is shifted by an amount ΔT . Disorder chaos is studied by introducing a perturbation ΔJ in the disorder, i.e.,

$$J_{ij} \rightarrow \tilde{J}_{ij} = \frac{J_{ij} + x\Delta J}{\sqrt{1 + \Delta J^2}} \quad (3)$$

which leaves the disorder distribution invariant. In Eq. (3) x is a Gaussian distributed random number with zero mean and standard deviation unity. To monitor the changes induced by the perturbations of the system, we compute the *chaoticity parameter* [11,12] given by

$$Q_{T_1, T_2} = \left[\frac{\langle q_{T_1, T_2}^2 \rangle}{\sqrt{\langle q_{T_1, T_1}^2 \rangle \langle q_{T_2, T_2}^2 \rangle}} \right]_{\text{av}} \quad (4)$$

for temperature chaos and by

$$Q_{\Delta J} = \left[\frac{\langle q_{J_{ij}, \tilde{J}_{ij}}^2 \rangle}{\langle q_{J_{ij}, J_{ij}}^2 \rangle} \right]_{\text{av}} \quad (5)$$

for disorder chaos, respectively.

In Eqs. (4) and (5) q^2 is the square overlap, Eq. (2), between two copies at different temperature or disorder. Here $\langle \dots \rangle$ represents a thermal average and $[\dots]_{\text{av}}$ represents a disorder average. In order to access low temperatures necessary to probe temperature chaos, we have used the parallel tempering [25,26] Monte Carlo method in combination with the equilibration test presented in Ref. [27]. Simulation parameters are listed in Table I.

Disorder and temperature chaos.—In what follows, we discuss how chaos can arise in spin glasses using the early arguments presented in Refs. [4,6,7,29]. Within the droplet theory framework [6,33], the low-lying excitations above the equilibrium state are obtained by flipping compact connected clusters of spins called droplets. A droplet of size ℓ has a fractal surface of dimension $d_s < d$, and its excitation free energy $F > 0$ is distributed via $P_T(F, \ell) = (\gamma(T)\ell)^{-\theta} \rho(F/\gamma(T)\ell^\theta)$, where $\rho(x)$ is a scaling function assumed to be nonzero at $x = 0$ and which decays to zero for large x . The free-energy exponent θ is argued on general grounds to be such that $0 < \theta \leq d_s/2$ and $\gamma(T)$ is the free-energy stiffness (which goes to zero at T_c). The droplet's entropy S can be written as $S = \sigma(T)\ell^{d_s/2}$, where σ is the entropy stiffness. Temperature chaos appears if the free energy of a droplet changes its sign when the temperature is modified. As noted in Refs. [6,7], the length scale at which this happens can be estimated by noting that the energy of a droplet does not change much with temperature. Therefore, if one considers a droplet at temperature T_1 with free energy $F(T_1)$, then at temperature $T_2 > T_1$

$$F(T_2) \approx F(T_1) + T_1 S(T_1) - T_2 S(T_2). \quad (6)$$

Because for typical droplets $F(T_1) = \gamma(T_1)\ell^\theta$ and $S = \sigma(T)\ell^{d_s/2}$, the free-energy excitation of such droplets becomes generally negative at temperature T_2 (so that the droplet has to be flipped) for length scales larger than the *chaotic length* [6,7] defined as

$$\ell_c = \left(\frac{\gamma(T_1)}{T_2 \sigma(T_2) - T_1 \sigma(T_1)} \right)^{1/\zeta} \quad \text{with} \quad \zeta = \frac{d_s}{2} - \theta. \quad (7)$$

TABLE I. Parameters of the simulation for each system size L . N_{samp} is the number of samples and N_{sw} is the total number of Monte Carlo sweeps used for equilibration for each of the $2N_T$ parallel tempering replicas for a single sample. An equal number of sweeps is used for measurement. The minimum temperature simulated is $T_{\text{min}} = 0.20$, the highest $T_{\text{max}} = 2.0$. For disorder chaos the disorder shifts used in Eq. (3) are $\Delta J = 0.001, 0.005, 0.02, 0.05, 0.1, 0.2$, and 0.5 . For temperature chaos we compute the overlap between T_{min} and T_i with $i \in \{2, \dots, N_T\}$ [28].

L	N_T	N_{samp}	N_{sw}
4	16	10 000	262 144
5	16	10 000	262 144
6	16	10 000	262 144
8	16	5000	1 048 576
10	22	2500	8 388 608

Usually, small temperature changes are studied such that $S(T_1) \approx S(T_2)$. Here, however, we do not use this approximation and since in the low-temperature phase, when one can define droplets, the entropy is proportional to \sqrt{T} [6,20], we write

$$\ell_c(T_1, T_2) \propto (T_2^{3/2} - T_1^{3/2})^{-1/\zeta}. \quad (8)$$

Equation (8) shows that when temperature is changed, equilibrium configurations are changed on scales greater than ℓ_c . Notice that by keeping the temperature dependence of the entropy, we obtain a slightly different scaling than usually considered [6,7], where a factor ΔT appears instead of $T_2^{3/2} - T_1^{3/2}$. While this makes no difference for small ΔT (which is the case in all simulations performed so far), this can be significant for temperature differences larger than the ones considered in this work. Similar arguments can also be applied to the case of a random perturbation in the disorder [6,7]—see, for instance, Ref. [34]—where one obtains

$$\ell_c(\Delta J) \propto \Delta J^{-1/\zeta}. \quad (9)$$

Considering system-size excitations, these arguments thus suggest that the chaoticity parameters defined in Eqs. (4) and (5) have the following scaling behavior

$$\begin{aligned} Q_{T_1, T_2}(L, T_1, T_2) &= F_T(L/\ell_c(T_1, T_2)), \\ Q_{\Delta J}(L, \Delta J) &= F_J(L/\ell_c(\Delta J)), \end{aligned} \quad (10)$$

where $F(x)$ is a function with $F(0) = 1$ that decays at large x . In what follows we test the aforementioned scaling relations via Monte Carlo simulations.

Numerical results.—The behavior of the chaoticity parameter for disorder chaos at zero temperature has recently

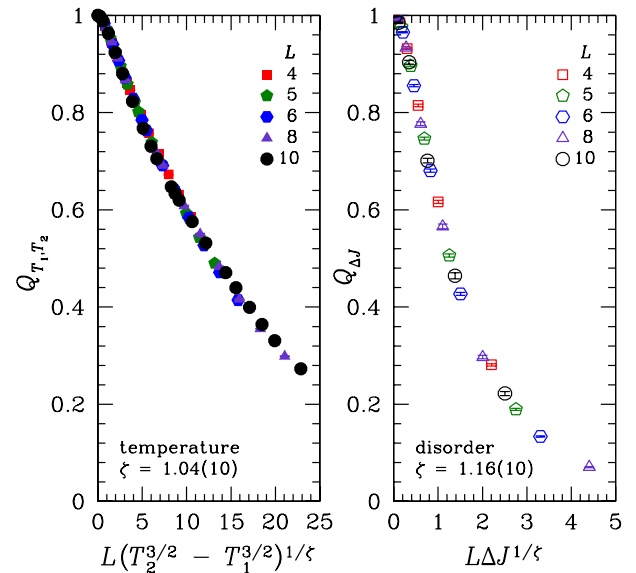


FIG. 1 (color online). Scaling plot of the chaoticity parameter for temperature chaos (left panel, $T_1 = 0.20$) and disorder chaos (right panel, $T = 0.20$) using L/ℓ_c as a scaling variable.

been studied in Ref. [34] (see also Ref. [35]) and perfectly satisfies the predictions of the droplet model. We thus concentrate here on finite temperatures where the scaling relations were only tested in the simulations of Refs. [11,12,21] in two and four space dimensions. We have performed low-temperature Monte Carlo simulations of the 3D Ising spin glass (see Table I). As can be observed in Fig. 1, scaling the data for disorder and temperature chaos according to Eqs. (10) works extremely well. The best scaling collapse determined by a nonlinear minimization routine [24] yields $\zeta \approx 1.04$ for temperature chaos and $\zeta \approx 1.16$ for disorder chaos, which is in rather good agreement with the accepted value $\zeta \approx 1.1$ from $d_s \approx 2.6$ [27,36] and $\theta \approx 0.2$ [33,37,38]; see Eq. (7). Notice that we have a good scaling of the data even when T_2 is larger than T_c . We have tested the temperature dependence of the exponent ζ and find that for $T \leq 0.5$ its value is practically independent of temperature, i.e., at $T = 0.20$ we are probing the low-temperature regime.

Renormalization group arguments also suggest that the temperature and disorder chaos effects are deeply related and characterized by the same universal scaling function [6,7,17–19] so that only nonuniversal prefactors differ. In Fig. 2, we thus superimpose the data for both perturbations presented in Fig. 1 by rescaling ℓ_c . Using $\zeta = 1.16$ for both perturbations and multiplying $\ell_c(\Delta J)$ by a factor $A \approx 8.7$, we obtain a rather good superposition in the low-temperature region, and we conclude that our data are thus compatible with the *equality* of the two scaling functions. From this ℓ -scale renormalization we also conclude

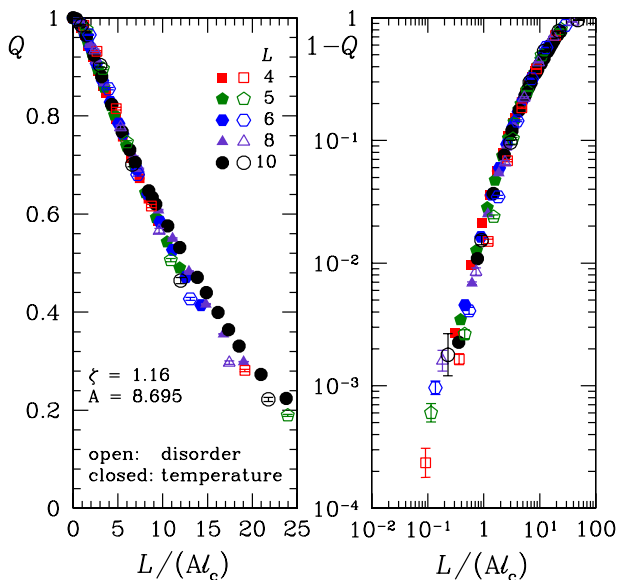


FIG. 2 (color online). Scaling plot of *both* disorder *and* temperature chaos. Left: chaoticity parameter Q as a function of L/ℓ_c . Scaling performed with $\zeta = 1.16$. Note that $\ell_c(\Delta T) \approx A\ell_c(\Delta J)$ with $A \approx 8.7$, i.e., disorder chaos appears at considerably shorter length scales than temperature chaos. Right: log-log plot of the same data, plotted as $1 - Q$, to illustrate the quality of the scaling.

that the length scale at which temperature chaos appears is approximately 10 times larger than the length scale needed for disorder chaos to appear, as has also been found in four space dimensions by Sasaki *et al.*; see Ref. [21]. Therefore, temperature chaos is harder to probe than disorder chaos, as has already been discussed within a Migdal-Kadanoff approach on spin glasses [20].

The superposition of the scaling functions shows deviations at larger temperatures. This is not surprising as assumptions made when deriving the scaling function are not valid for high T . For example, the \sqrt{T} dependence of the entropy or the very existence of droplets is only valid for $T \leq T_c$ [39]. We thus believe that to perform a definitive test of universality of the scaling functions, very large system sizes at low temperatures with small temperature changes should be used.

We also study the behavior of the scaling function. It decays as $(\ell_c/L)^{d/2}$ for strong chaos (when $\ell_c/L \leq 1$) [34]. However, in the limit $\ell_c/L \geq 1$, we obtain $1 - Q(x) \propto x^{3\zeta/2}$ which differs from the $1 - Q(x) \propto x^\zeta$ behavior found at zero temperature in Ref. [34]. This shows that the scaling function can have a more subtle behavior than what is naïvely expected from simple domain-wall arguments [21,40]. Note that the results remain unchanged if one takes the disorder average of the different overlaps in Eq. (4) *independently*, as done in Eq. (11) of Ref. [21].

Finally, to better illustrate the mechanism of chaos, we study the distribution of the chaoticity parameter over the disorder for temperature chaos, i.e., we compute the chaoticity parameter Q as defined in Eq. (4) without the disorder average, and bin the data for different choices of the disorder to compute the distribution $P_L(Q_{T_1, T_2})$. According to the droplet model, in the weak chaos regime (where $\ell_c > L$), temperature chaos can manifest itself even on small length scales, but only for rare regions of space [17]. This means that even for small ΔT , when Q is very close to unity, the distribution is broad and rare samples with lower values are expected. Figure 3 shows the distribution $P_L(Q_{T_1, T_2})$ for $L = 10$ for $T_1 = 0.2$ and different $T_2 = T_1 + \Delta T$ [28]. Even for modest ΔT , rare but large changes are clearly observed. This illustrates the weak chaos scenario presented in Ref. [17]: temperature chaos (at least in the weak regime) is not due to moderate changes in all samples, but rather due to larger changes in a few rare samples.

Conclusions.—We have studied numerically disorder and temperature chaos in 3D Ising spin glasses and show that both disorder as well as temperature chaos are well described within a scaling or droplet description. In particular, we find that the scaling variables have to be modified as done in Eq. (8) when the difference in temperature is large. In addition, we show that the weak chaos regime is dominated by rare events where system-size droplets are flipped. This has direct experimental implications because the weak chaos regime has been argued to account in a *quantitative* way for the memory and rejuvenation effects

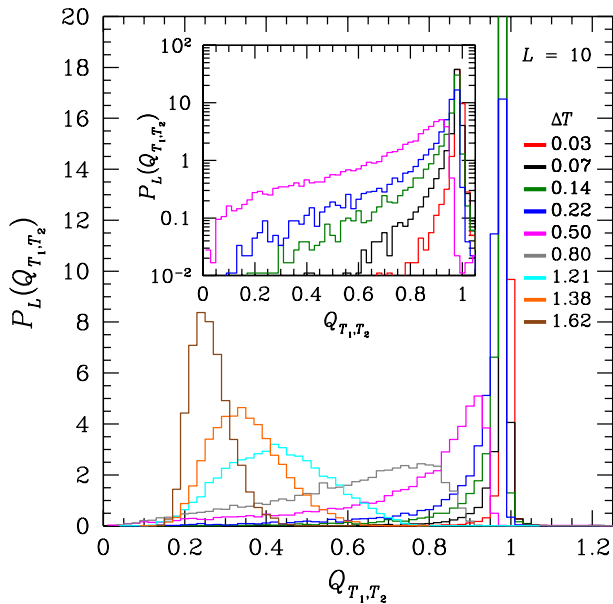


FIG. 3 (color online). Distribution of the chaoticity parameter over different realizations of the disorder for $L = 10$ with $T_1 = 0.2$ and $T_2 = T_1 + \Delta T$ [28]. In the case of small ΔT rare samples have very low values of Q while most of them remain unchanged ($Q = 1$). The inset shows a linear-log plot of the data for the smallest values of ΔT for which $T_1 < T_2 < 2T_c/3$. For all T_2 the distribution has a single peak, unlike for the random-energy models with entropic fluctuations [30,31].

[10]. Finally, we show that temperature and disorder chaos might be described by similar scaling functions in the low-temperature regime, thus providing compelling evidence for the presence of a chaotic temperature dependence in spin glasses. This has also recently been proven for mean-field systems [32,41]. This mechanism is also responsible for step-wise responses that could in principle be observed experimentally in mesoscopic systems [32,41]. Nevertheless, this behavior might change for larger system sizes and thus we propose to revisit the problem with better models [42]. Our findings will help interpret experiments on rejuvenation and memory effects in spin-glasses and other materials.

We thank A. Billoire, J.-P. Bouchaud, T. Jörg, M. Sasaki, H. Yoshino, A. P. Young, and L. Zdeborová for discussions. The simulations have been performed on the Hreidar and Gonzales clusters at ETH Zürich.

[1] S.F. Edwards and P.W. Anderson, *J. Phys. F* **5**, 965 (1975).
 [2] M. Mézard, G. Parisi, and M.A. Virasoro, *Spin Glass Theory and Beyond* (World Scientific, Singapore, 1987).
 [3] *Spin Glasses and Random Fields*, edited by A.P. Young (World Scientific, Singapore, 1998).
 [4] S.R. McKay, A.N. Berker, and S. Kirkpatrick, *Phys. Rev. Lett.* **48**, 767 (1982).
 [5] G. Parisi, *Physica (Amsterdam)* **124A**, 523 (1984).

[6] D.S. Fisher and D.A. Huse, *Phys. Rev. Lett.* **56**, 1601 (1986).
 [7] A.J. Bray and M.A. Moore, *Phys. Rev. Lett.* **58**, 57 (1987).
 [8] P. Nordblad and P. Svendlidh, in *Spin Glasses and Random Fields*, edited by A.P. Young (World Scientific, Singapore, 1998).
 [9] V. Dupuis, E. Vincent, J.-P. Bouchaud, J. Hammann, A. Ito, and H.A. Katori, *Phys. Rev. B* **64**, 174204 (2001).
 [10] P.E. Jönsson, R. Mathieu, P. Nordblad, H. Yoshino, H.A. Katori, and A. Ito, *Phys. Rev. B* **70**, 174402 (2004).
 [11] M. Ney-Nifle and A.P. Young, *J. Phys. A* **30**, 5311 (1997).
 [12] M. Ney-Nifle, *Phys. Rev. B* **57**, 492 (1998).
 [13] A. Billoire and E. Marinari, *J. Phys. A* **33**, L265 (2000).
 [14] A. Billoire and E. Marinari, *Europhys. Lett.* **60**, 775 (2002).
 [15] I. Kondor, *J. Phys. A* **22**, L163 (1989).
 [16] D.S. Fisher and D.A. Huse, *Phys. Rev. B* **43**, 10728 (1991).
 [17] M. Sales and H. Yoshino, *Phys. Rev. E* **65**, 066131 (2002).
 [18] R.A. daSilveira and J.-P. Bouchaud, *Phys. Rev. Lett.* **93**, 015901 (2004).
 [19] P. le Doussal, cond-mat/0505679.
 [20] T. Aspelmeier, A.J. Bray, and M.A. Moore, *Phys. Rev. Lett.* **89**, 197202 (2002); T. Rizzo and A. Crisanti, *Phys. Rev. Lett.* **90**, 137201 (2003).
 [21] M. Sasaki, K. Hukushima, H. Yoshino, and H. Takayama, *Phys. Rev. Lett.* **95**, 267203 (2005).
 [22] R.N. Bhatt and A.P. Young, *Phys. Rev. B* **37**, 5606 (1988).
 [23] E. Marinari, G. Parisi, and J.J. Ruiz-Lorenzo, *Phys. Rev. B* **58**, 14852 (1998).
 [24] H.G. Katzgraber, M. Körner, and A.P. Young, *Phys. Rev. B* **73**, 224432 (2006).
 [25] K. Hukushima and K. Nemoto, *J. Phys. Soc. Jpn.* **65**, 1604 (1996).
 [26] E. Marinari, G. Parisi, J. Ruiz-Lorenzo, and F. Ritort, *Phys. Rev. Lett.* **76**, 843 (1996).
 [27] H.G. Katzgraber, M. Palassini, and A.P. Young, *Phys. Rev. B* **63**, 184422 (2001).
 [28] Temperatures T_2 in Eq. (4): 0.27, 0.34, 0.42, 0.50, 0.60, 0.70, 0.82, 0.94, 1.00, 1.20, 1.34, 1.50, 1.66, 1.82, 2.00.
 [29] Note similar arguments can be used for mean-field systems [30–32] leading to similar conclusions.
 [30] F. Krzakala and O.C. Martin, *Eur. Phys. J. B* **28**, 199 (2002).
 [31] I. Kurkova, *J. Stat. Phys.* **111**, 35 (2003).
 [32] T. Rizzo and H. Yoshino, *Phys. Rev. B* **73**, 064416 (2006).
 [33] A.J. Bray and M.A. Moore, *J. Phys. C* **17**, L463 (1984).
 [34] F. Krzakala and J.-P. Bouchaud, *Europhys. Lett.* **72**, 472 (2005).
 [35] H. Rieger, L. Santen, U. Blasum, M. Diehl, M. Jünger, and G. Rinaldi, *J. Phys. A* **29**, 3939 (1996).
 [36] M. Palassini and A.P. Young, *Phys. Rev. Lett.* **85**, 3017 (2000).
 [37] W.L. McMillan, *Phys. Rev. B* **30**, R476 (1984).
 [38] A.K. Hartmann, *Phys. Rev. E* **59**, 84 (1999).
 [39] M. Nifle and H.J. Hilhorst, *Phys. Rev. Lett.* **68**, 2992 (1992).
 [40] F. Scheffler, H. Yoshino, and P. Maass, *Phys. Rev. B* **68**, 060404(R) (2003).
 [41] H. Yoshino and T. Rizzo, cond-mat/0608293.
 [42] H.G. Katzgraber, M. Körner, F. Liers, and A.K. Hartmann, *Prog. Theor. Phys. Suppl.* **157**, 59 (2005).